SUPERCONDUCTING CAVITIES

G. Bisoffi
INFN, National Laboratories, Legnaro, Italy

Abstract
The main features of superconducting cavities are discussed. Their advantages with respect to the normal-conducting cavities as well as the basics of RF surface resistance are treated first. Then, design, construction and surface-treatment issues are addressed, together with the particular methods used to assess the quality factor and accelerating field of superconducting cavities. Anomalous losses, related to the surface electric and magnetic fields, are discussed in detail. A description of the present state of the art concludes the lecture notes.

1 INTRODUCTION

The interest in superconducting (SC) resonators shown by the community of elementary particle physicists is steadily increasing. Colliding beam storage rings, recirculating linacs and free electron lasers gain significantly from the high energy, high intensity and small emittance that can be achieved by using SC cavities. On the low-energy side in continuous wave (CW) mode, the SC boosters of heavy-ion Van de Graaf accelerators can maintain the excellent beam properties of their injectors, allowing them to probe nuclear structure around the Coulomb barrier between projectile and targets of all elemental species. On the application side (e.g. material studies, transmutation of nuclear wastes and subcritical reactors), SC-resonator-based accelerators of high-intensity protons (at least for the medium and high energies) were quite recently considered.

The basic aspects of SC resonators are described in this lecture. Their main advantages with respect to the normal-conducting (NC) option will be presented (Section 2) and some fundamental aspects of RF superconductivity will be recalled (Section 3). The design and construction of SC resonators (Section 4) as well as measurement techniques used to assess their performance (Section 5) will be reviewed. To conclude the lecture, the most important limitations to accelerating fields currently attainable will be summarized (Section 6) and some of the most recent advances in the field will be highlighted (Section 7). Some important ancillary topics, such as high power and high order mode couplers, cavity frequency stabilization techniques, especially with respect to microphonics and Lorenz-force detuning, can not be treated in a one-hour lecture. The interested reader should consult the more specialized literature [1].

2 ADVANTAGES OF SUPERCONDUCTING CAVITIES

The most striking advantage in using superconducting cavities is the possibility to work in a CW mode or at least at a significantly higher duty cycle than with NC cavities. Power dissipation on the wall of SC cavities is typically 10^5 times smaller than in the NC case. This is expressed in terms of the quality factor Q_0, the universal figure of merit of resonators, which is the ratio between the stored energy U and the power dissipated by the cavity P_c in one RF cycle of the resonant angular frequency ω_0:

$$Q_0 = \frac{\omega_0 U}{P_c} \, .$$

If we take the linac definition of shunt impedance per unit length, $r_a = V_c^2/P_c'$, we can easily see that the dissipated power per unit length in a linac P_c' can be expressed as:

$$P_c' = \frac{E_{acc}^2}{\left(\frac{r_a}{Q_0}\right) Q_0} \tag{1}$$

where r_a/Q_0 is the geometric shunt impedance in Ω/m, which depends basically on the structure geometry. The main attraction of superconductivity for RF cavities can be expressed in terms of P_c'. For example, an accelerating field of 5 MV/m typically corresponds to a power dissipation of $\sim$ 40 W/m for SC structures ($Q_0 = 2 \times 10^9$) versus $\sim$ 4000 kW/m for NC structures ($Q_0 = 2 \times 10^4$). The latter is not a practical value since, beyond $\approx$ 100 kW dissipation in a Cu cell, heat removal becomes a concern and problems related to the temperature (T) increase (e.g. mechanical stress, thermal expansion, outgassing) become prohibitive.

SC structures are not intrinsically limited by the cooling capability when pushing to higher E_{acc} values. They are limited rather by anomalous losses (e.g. field emission or quenches), which nowadays imposes an ultimate limit at $E_{acc} \sim 40$ MV/m (see Sections 6 and 7). Fields as high as these can also be reached with NC cavities, but only for microseconds because of the prohibitive power requirements.

Clearly, as far as the overall mains power is concerned, the situation is less advantageous than previously depicted, because of the refrigeration cost. Carnot efficiency $\eta_c = T_2/(T_1 - T_2), T_1 = 300$ K and $T_2 = 4.2$ K, as well as thermodynamic efficiency $\eta_{th} \approx 0.3$ (ratio of the compressor power needed for the ideal reversible case to the real power) must be considered, giving

$$\eta = \eta_c \eta_{th} = 4.5 \times 10^{-3} \, . \tag{2}$$

On the NC side, the efficiency of the klystron source (typically 0.5) must be considered. Eventually, an AC power saving factor of $\sim$ 200 is obtained for SC cavities, just taking cavity operation into account. This is true, for example, for heavy-ion structures, where the beam current is negligible. However, including the power necessary to accelerate, say, a 5 mA beam (and benefiting from a factor 3 higher field with SC cavities) the cavity-plus-beam power load is significantly higher and the power saving factor reduces to about 5, which is still a significant value.

The possibility of increasing inter-cell iris openings and making them rounded is another important advantage of SC cavities in many applications. The associated decrease in the cavity shunt impedance is not a concern, since it is dominated by the much larger quality factor. One advantage is that the cavity impedance Z can be typically 10 times smaller, which pushes the threshold of beam instabilities to higher currents I (the growth time of instabilities being $\tau_{inst} \propto 1/ZI$). SC cavities are also interesting for intense proton beam linacs, since beam halos are less prone to scrape on accelerator components and activate them.

3 RF SURFACE RESISTANCE AND ULTIMATE FIELD LIMITS

3.1 The RF resistance of a superconducting surface

The microwave surface resistance of normal metals is expressed by $R_s = \sqrt{\pi f \mu_0/\sigma} = 1\sigma\delta$, σ being the electrical conductivity, f the RF and δ the penetration of the EM fields (skin depth), $\delta = 1/\sqrt{\pi f \mu_0 \sigma}$. At low T and high frequency (σ increases by lowering the temperature) δ may become shorter than the mean free path of an electron. In this case the electrons spend only part of the time between collisions in the field penetrated region. Consequently the electrons become less effective in shielding the field and, somehow counter-intuitively, longer mean free paths lead to higher surface resistance than expressed above ('anomalous skin effect').

In computing the anomalous-skin-effect limit for copper at microwave frequencies and cryogenic temperatures, one can see that, although the DC conductivity increases by a factor 100, the anomalous skin effect allows only a decrease of a factor 6 in the surface resistance. This shows that it is definitely not convenient to cool an NC metal to cryogenic temperatures.

The SC regime is completely different. Following the London 'two-fluid' model [2], we can view the situation for superconductors at $T < T_c$ as the coexistence of two fluids, a superfluid of paired electrons (Cooper pairs) and the normal fluid of free electrons: a 'supercurrent' and a normal current flow in

parallel. In this situation all DC current is carried by the supercurrent and the DC resistance of a superconductor below T_c is exactly zero. In AC regime, however, the surface resistance of a superconductor is always larger than zero, albeit very small compared to NC metals. In fact, although Cooper pairs move without resistance even when exposed to RF fields (no power dissipation) they have inertia. This means that the time-varying surface magnetic field $H_s \cos \omega t$ (H_s being the magnetic field at the metal surface and ω the angular frequency) must extend beyond the surface of the material to create the forces which can provide back-and-forth acceleration of the pairs and oppose the RF surface currents. This is expressed in terms of an induced electric field

$$E \propto \frac{\mathrm{d}H}{\mathrm{d}t} \propto \omega H_s \tag{3}$$

inside the material. Once time-varying electric fields are present in the skin layer, they will act on the unpaired electrons as well and the latter can interact with the lattice and produce losses, following the anomalous skin effect. The equivalent 'superconducting skin depth' is about as large as the London penetration depth λ_L (depth of penetration of the magnetic field in a superconductor, ranging from 15 to 110 nm, depending on the particular metal), and is about a factor 100 smaller than δ.

For frequencies below 10 GHz and $T < T_c/2$, experimental data are well described by the empirical relation

$$R_s = A \, \frac{\omega^2}{T} \, e^{-\alpha \frac{T_c}{T}} + R_{res} \, , \tag{4}$$

where A and α depend on material parameters [3].

The most noticeable features of this expression are that R_s increases with the square of the RF and decreases exponentially with temperature. This suggests that high-frequency cavities (e.g. 1.5 GHz) need to be cooled below T = 2 K to give acceptably low surface resistance. The first term of this expression, coming from the two-fluid model (also called Bardeen–Cooper–Schrieffer, or BCS resistance), is in excellent agreement with experimental results for frequencies below $\sim$ 10 GHz, which is also the range of practical interest for nearly all SC cavities.

Figures showing the temperature dependence of surface resistance of niobium (Nb) at, for example, 3 GHz nicely demonstrate the existence of the residual resistance which appears in the formula above (see, for example, Fig. 1). R_{res} is temperature-independent and accounts for residual loss limitations of actual SC cavities, which will be discussed in Section 6.1. Typical values of R_{res} are 10 to 20 nΩ. R_{res} is usually the dominating resistance limitation in low-frequency low-β resonators (f = 50 to 150 MHz), for which simpler cryogenic operation at 4.2 K is sufficient.

3.2 Intrinsic field limitations in SC cavities

When a magnetic field is present at the SC to NC phase transition (as is the case when raising the EM fields in a cavity), a latent heat exists which is related to a discontinuity in entropy. As a result the transition requires some finite amount of heat input to compensate for the change in entropy. NC nucleating centres are created, beyond T_c, in an overall SC regime.

For typical SC cavity frequencies, the wave period ($\sim 10^{-9}$ s) is much shorter than the time it takes to creates the nucleation centres ($\sim 10^{-6}$ s). Therefore, it seems possible for the SC state to survive beyond H_C, up to a 'superheating' critical field H_{sh}, exceeding H_C for type I superconductors and H_{C1} for type II superconductors [2]. Nowadays H_{sh} is rated as the maximum theoretical limitation for SC resonators.

A dependence of H_{sh} on the ratio $\kappa = \lambda_L/\xi$ (where ξ is called the 'coherence length' and represents a sort of spatial extension of the Cooper pair which carries the supercurrent) was calculated [5] with a phenomenological theory of superconductivity, showing that

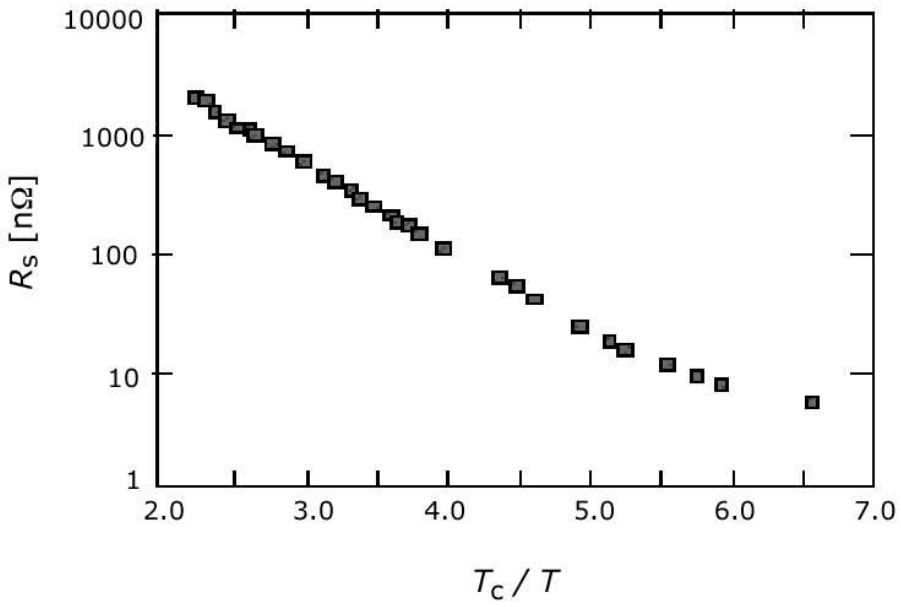

Fig. 1: Surface resistance of a 3 GHz niobium sheet cavity (RRR = 40) plotted against T_c/T. The residual resistance is 4 nΩ [4].

$$\begin{aligned} H_{sh} &\approx \frac{0.89}{\sqrt{k}} H_C \qquad \text{for } \kappa \ll 1 \ , \\ H_{sh} &\approx 1.2\, H_C \qquad \text{for } \kappa \sim 1 \ , \\ H_{sh} &\approx 0.75\, H_C \qquad \text{for } \kappa \gg 1 \ . \end{aligned} \tag{5}$$

H_C has been exceeded in some cases, while H_{sh} has never been exceeded experimentally, which seems to be an experimental indication that H_{sh} is the fundamental limit to the performance of an SC resonator. For Nb at T = 0, for example, H_C = 200 mT and H_{sh} = 240 mT.

There exists no known theoretical limitation to the peak surface field, E_{pk}, whereas the well known, often encountered, practical limitations connected with electron field emission will be discussed in Section 6.

4 DESIGN, CONSTRUCTION, AND TREATMENT ISSUES

4.1 Design

When addressing the basic design of a new SC resonator, a small flowchart of the most significant issues could be followed.

4.1.1 β and frequency

The bunch length determines an upper limit to the frequency of a resonant structure, which should be much smaller than the wavelength. To gain as much as possible from the accelerating voltage present on the various gaps of a resonant structure, the bunch should cross them while the electric field is closest to its maximum value. Consequently the resonant frequency f_0 has to be related to the inter-gap distance d and the bunch velocity βc through

$$f_0 d \approx \frac{\beta c}{2} \ . \tag{6}$$

At low values of β, the need of useful accelerating lengths ($\beta\lambda \sim 5$ to 10 cm) implies that the wavelength λ has to be large and therefore that the resonant frequency has to be small. Low-β resonators hence tend to be large in size (see two examples in Fig. 2). The condition $\beta \sim 1$ (typical of electron cavities) calls instead for frequencies in the range of 300 to 3000 MHz for accelerating lengths of 5 to 40 cm.

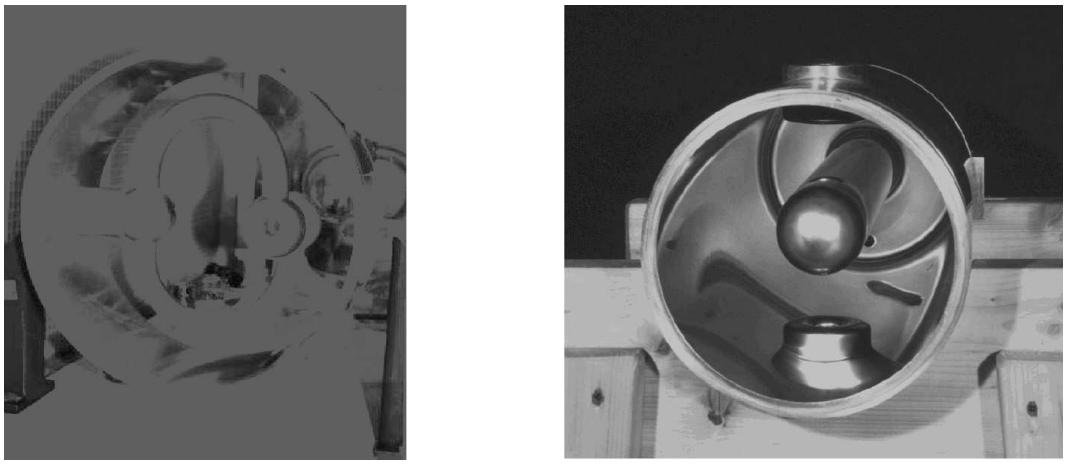

Fig. 2: Two examples of low-β SC resonators for heavy ions: a split-loop resonator (left) and a quarter wave resonator (right)

Within the somewhat broad frame mentioned above, a lower resonant frequency would imply smaller BCS resistance, calling however for a larger cryostat and higher associated fabrication costs. Larger surface cavities, moreover, increase the probability of introducing surface defects, which are a source of lower performance.

4.2 Number of gaps

As far as heavy-ion SC structures are concerned, it is convenient to build them with a small number of gaps, so as to accommodate the largest possible acceptance in the natural spread of β-values coming from the typical injectors of these machines.

This inconvenience does not arise in the design and production of SC cavities for $\beta \sim 1$, in which multigap resonators are the natural choice. They are built as a chain of N quasi-pillbox cavities, coupled through the iris openings. While the angular frequency of the lowest mode of a single simple pillbox without beam ports is $\omega_0 = 2.405\ c/a$ (a being the pillbox radius), which approximately sizes the cavity as a function of the chosen frequency, with N coupled cells the angular frequency is

$$\omega_q = \omega_0(1 + K\ \cos\ \alpha_q)\ , \tag{7}$$

where $\alpha_q = \frac{q\pi}{N}(q = 1, ...,\ N)$ and K is the coupling factor between adjacent cells, dependent on the iris diameter and geometry. Among the N fundamental resonant frequencies, it is useful to operate in the 'π' mode $(q = N)$, which has the highest shunt impedance. The field pattern of the π-mode is shown in Fig. 3.

Lower manufacturing costs, more efficient use of the accelerating voltage, smaller fringing field effects and fewer inter-cavity drift spaces are points in favour of having a *large number of coupled cells*.

A flatter electric field from cell to cell and lower overall power from the input coupler are points in favour of a *small number of coupled cells*.

The choice depends on each application.

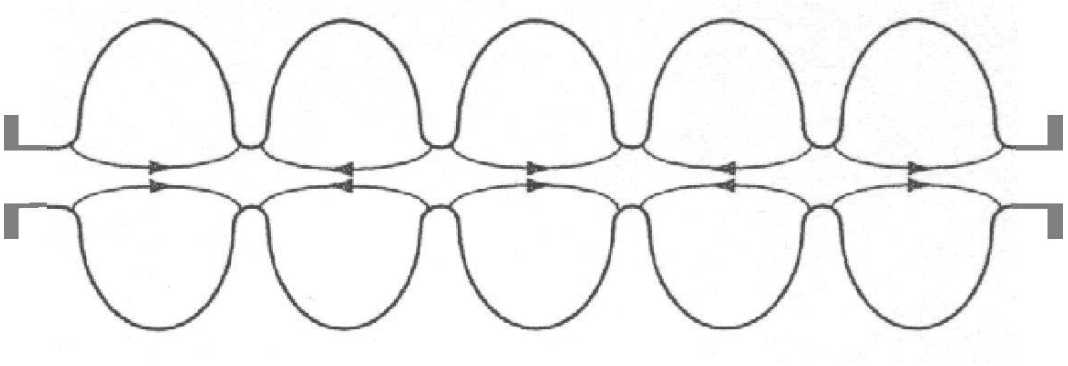

Fig. 3: π-mode of a β = 1 multicell cavity

4.3 Iris aperture

A large and rounded iris opening will increase uniformity in the field distribution from cell to cell, and will also offer a smaller impedance to the beam (implying better beam quality and larger currents).

On the other hand the shunt impedance will be lower (more refrigeration power needed) and the accelerating field will be smaller. Again the particular application will indicate the ideal choice.

4.4 Construction technologies

4.4.1 Full niobium

Once the geometric design of an SC cavity has been basically fixed, the material must be chosen, which is associated with a particular construction expertise.

Pure Nb is the most widely used material, supplied in sheets then shaped, cut and joined by electron-beam welding (EBW). This will be considered as the 'default' choice in the following discussion on construction and treatment. Niobium is a good choice since it has a quite high critical temperature (T_c = 9.2 K) and lower RF resistance, see Eq. (4). Expertise in the production of very pure (high residual resistance ratio or RRR) sheets and bars, the shaping of cavity parts and EBW has reached a high level and can be applied to almost any complex geometry with little additional R&D.

High-RRR Nb is obtained by boiling out impurities in an electron-beam furnace, in several stages, at a base pressure of 10^{-4} to 10^{-5} Torr. C, N, H and O are quite efficiently removed in this way. These are by far the worst impurities from the point of view of electron mobility. High-RRR Nb ingots are laminated in subsequent stages, annealed, and delivered by the supplier.

Deep drawing or drop-hammer-forming, using dies made out of aluminium can accomplish forming. These dies are easy to make and any aluminium sticking on the Nb surface during machining can be removed by subsequent chemical etching. Trimming Nb parts to their final pre-EBW shape should ideally be done by a computer-controlled milling machine, operated at very low speed to avoid heating up the part beyond 100°C (otherwise they would again be contaminated by gaseous impurities in the bulk). Prior to EBW, components must be degreased and lightly etched on the edges to be welded by a buffered chemical polishing (BCP) solution, made out of one part hydrofluoric acid, one part nitric acid and two parts phosphoric acid (the so-called 1:1:2 solution). In this process 5 to 20 mm material removal seems sufficient.

Typical EBW parameters are a pressure below 2 to 4 $\times$ 10^{-5} Torr in the welding chamber, and a 50 kV/ 40 mA electron-beam current at 1 cm/min velocity on the joint (usually the electron beam stays fixed and the parts are moved in the EBW vacuum chamber). Experience with EBW has shown that a full-penetration joint with a smooth 'underbead' (the welded part opposite the beam side) can be obtained by either defocusing the electron beam or by making it oscillate with an elliptical or rhombic pattern along

the joint. If EBW is performed from the 'inside' of the resonator being built, full penetration is not an issue and the EBW parameters are somewhat more relaxed.

Rough tuning to the final frequency (after carefully predicting subsequent changes due to chemical etching, resonator evacuation and temperature change) is usually performed at the end of the construction procedure. Each cell of a multicell cavity, for example, can be squeezed or stretched by gripping the irises, which also improves the field flatness as desired.

After the final geometry has been obtained, final purification of the Nb by means of solid-state gettering might be applied [6]. This can increase the RRR up to values of the order of 1000.

4.4.2 Alternatives to full electron-beam-welded niobium

Construction technologies alternative to solid Nb are discussed in the following.

For low-β applications, for example, the residual resistance almost always dominates the BCS resistance: lower T_c and easier cryogenic operation at 4.2 K can be allowed. *Electroplating lead onto a copper substrate* is in this case a simple, less expensive choice, which can also be adapted to rather complicated geometry [7].

- Sputtering of Nb onto a Cu substrate is becoming a more and more interesting alternative to solid Nb, since performances have been demonstrated to be almost comparable. The technique has been developed with success for both $\beta > 0.8$ [8], [9] and $\beta = 0.13$ cavities [10]. One can save on the significant cost of the high-RRR Nb and profit from the excellent thermal stabilization offered by the Cu substrate, thanks to which quenches are virtually never the field limit for Nb-sputtered resonators. A value of $RRR \sim 30$ can be reached, which minimizes the BCS contribution to surface resistance. Nb-sputtered cavities still generally suffer from a non-negligible drop of the quality factor versus increasing accelerating field. It is being discussed at present whether this is related to the weak links between SC grains on the cavity surface or to problems of the Nb-to-Cu interface.
- Nb_3Sn coatings (obtained by evaporated and heated up Sn on a pure Nb surface) are extremely promising because of their higher critical temperature (T_c = 18 K). $E_{acc} \sim 15$ MV/m is the present practical limitation.
- High-T_c superconductors, such as YBCO, might be interesting if epitaxial films are made to grow on a monocrystalline substrate [11], in which case the residual resistance is not expected to increase with the RF field. However, the development of this technology is still limited to samples of very small area.
- Within the full-Nb choice, promising techniques are being developed in building seamless resonators by either hydroforming [12] or spinning [13] (Fig. 4). Reducing EBW costs seems mandatory in future high-energy accelerators, like TESLA, where a significant reduction in the cost of the whole machine could be thus obtained. Seamless resonators were also developed in Cu, then sputtered with an SC Nb layer.

4.5 Surface treatments

Coming back to full Nb, the interior of the surface needs to be chemically etched (e.g. by the same 1:1:2 solution mentioned above) so as to remove the layer damaged during the mechanical construction. It has been shown [14] that removal of 100 μm is, in most cases, appropriate. An increase of the bath temperature beyond 18 to 20°C might trap H in the material bulk, affecting the final quality factor (see Section 6.1.2): hence temperature control appears to be a very important precaution.

Complementary to BCP, electropolishing (EP) has recently gained great attention since it seems necessary to adopt it in order to push the maximum accelerating fields of multicell cavities far beyond 25 MV/m [15]. In EP, Nb is the anode, the cathode is made of Al and the electrolyte consists of a

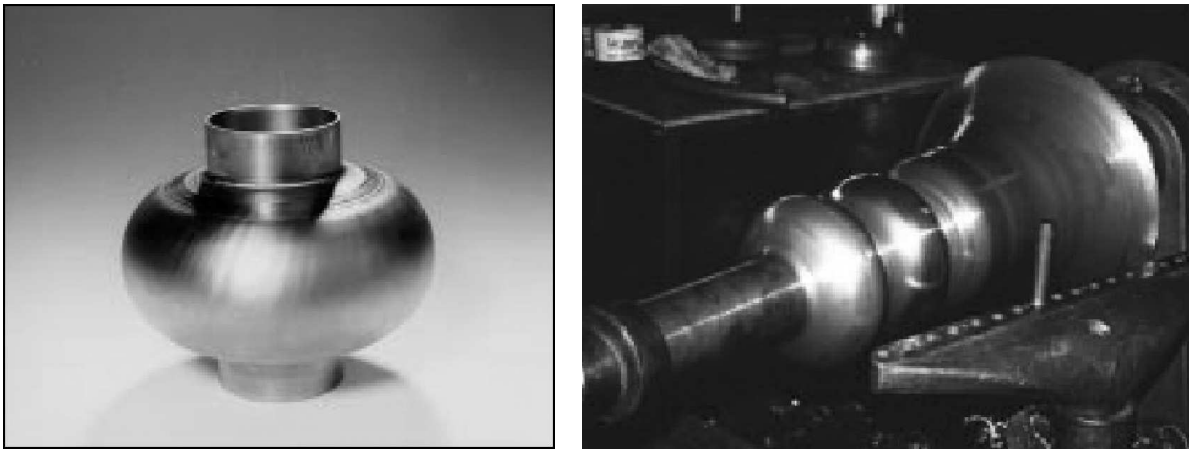

(a) (b)

Fig. 4: Hydroforming [12] and spinning [13] represent the most advanced technologies to produce niobium resonators without electron-beam welding.

solution of H_2SO_4 and HF. The cavity is gently rotated during the treatment. The smooth mirror-like surface finishing seems responsible for the lower resistance, at grain boundaries, than that achievable with the rather rough BCP.

After polishing, rinsing with pure water (ρ = 18 MΩ-cm) for several hours is necessary. High-pressure water rinsing (HPWR) with ultra-pure water is a recent and well-established technological development. 60 to 100 bar water jets, sprayed through 0.2 mm nozzles, seem to remove the most adherent contaminants and might be beneficial to the removal of defects in regions of both high magnetic field (quenches) and high electric field (field emission).

After HPWR, the SC cavity must be dried and assembled with the utmost care in a clean environment (class 10 or 100), so that no dust is allowed to settle on the SC surface and become the cause of field emission during tests.

5 MEASUREMENT OF THE PERFORMANCE OF A SUPERCONDUCTING CAVITY

The quality factor Q gives an overall assessment of the cavity performance, since all power losses are taken into account. On some occasions, if the results need to be improved, investigations of sources of local power dissipations are possible by other means (e.g. temperature mapping [16], [17]).

For Q measurements, a resonator is equipped with an input coupler port, driving the power coming from the RF source, and a pickup port, which typically samples a small fraction of the resonator stored energy. The TEM line field is coupled to the cavity field. The further in the position of the coupler, the stronger the coupling between the field coming from the RF drive and the superimposed cavity field components in the coupler port. Since the cavity field decays exponentially in the port it is possible to adjust the position of the coupler mechanically for a critical matching of the two fields (the line sees the cavity as a perfectly matched load).

It is worth underlining that the Q_0 value of an SC cavity cannot be measured through the formula $Q_0 = f_0/\Delta f$ (f_0 being the cavity resonant frequency and Δf the resonance bandwidth) since the latter—at a Q_0 value of 10^9 or higher—could be as small as a few hertz or less. Hence the evaluation of the decay time of the cavity stored energy is the only accurate measurement technique.

5.1 Definitions

Let us recall the main parameters involved in the assessment of the quality factor, obtained from the decay time of the cavity stored energy, once the cavity is fed by rectangular forward power pulses. At RF drive switched-off, the total power lost by the cavity (P_t) is that dissipated by the cavity itself (P_c) plus that emitted from the coupler (P_e) and the pickup (P_{pu}) ports: $P_t = P_c + P_e + P_{pu}$.

While the intrinsic Q_0 of a resonator is defined as $Q_0 = \omega_0 U/P_c$ (ω being the angular frequency and U the stored energy), we can define a loaded quality factor as $Q_L = \omega_0 U/P_t$. A measurement of Q_L can be deduced by a measurement of the decay time of the cavity stored energy U, through

$$\frac{\mathrm{d}U}{\mathrm{d}t} = -P_t = -\frac{\omega_0 U}{P_t}\ , \ \text{giving}\ U(t) = U_0 e^{-\frac{\omega_0 t}{Q_L}}\ \text{and}\ \tau_L = \frac{Q_L}{\omega_0}.$$

However Q_0 (and not Q_L) is the interesting parameter in order to assess the resonator performance; we can extract it through

$$\frac{1}{Q_L} = \frac{P_c}{\omega_0 U} + \frac{P_e}{\omega_0 U} + \frac{P_{pu}}{\omega_0 U} = \frac{1}{Q_0} + \frac{1}{Q_e} + \frac{1}{Q_{pu}} = \frac{1}{Q_0}(1 + \beta_e + \beta_{pu})\ , \tag{8}$$

where the coupler and pickup quality factors Q_e and Q_{pu} are contextually defined, together with the coupling factors β_e and β_{pu} of the two antennas,

$$\beta_e = \frac{Q_0}{Q_e} = \frac{P_e}{P_c}\ \text{and}\ \beta_{pu} = \frac{Q_0}{Q_{pu}} = \frac{P_{pu}}{P_c}\ .$$

The only role of the pickup coupler is that of sampling a portion of the stored energy, which can then be calibrated to give indications on the entity of the accelerating field: it is hence reasonable to design it such that $\beta_{pu} \ll 1$. Hence in the following we shall take $\beta = \beta_e$ and consider the coupler-plus-cavity ensemble as an overall driven harmonic oscillator (at the resonant frequency of the cavity), the steady state and the transient behaviour of which can be investigated.

5.2 Response of a cavity to rectangular RF pulses

A complete treatment of the equivalent circuit and of the response of a resonator to rectangular forward pulses is given in Ref. [18], in which the switching-on and switching-off conditions are treated as particular examples.

A very useful expression of the reflected power is derived from the switching-on treatment:

$$P_r = \left[1 - \frac{2\beta}{1+\beta}\left(1 - e^{-\frac{t}{2\tau_L}}\right)\right]^2\ . \tag{9}$$

The behaviour of the reflected power during switch-on regime can be viewed on an oscilloscope, together with the pickup signal and the signal from the forward power. This gives an immediate visual assessment of the coupling strength and provides a direct measurement of its value with sufficient accuracy.

At β = 1 and at resonance (at $t = \times$) $P_r = P_e$ = 0, meaning that all forward power goes into cavity power (*critical coupling*) and the cavity is a perfectly matched load to the transmission line. This condition is normally the preferred one for Q_0 measurements. The loaded decay time τ_L can be measured by either the reflected (emitted) or the pickup signal after having switched off the forward-power rectangular pulse:

$$Q_0 = \omega_0\ \tau_L(1+\beta) = 2\omega\tau_L\ (\text{in critical coupling})\ . \tag{10}$$

5.3 Q_0 measurements require frequency locking

Given the extremely narrow bandwidth, it is necessary to keep the circuit frequency locked to the resonant frequency f_0 in the course of the measurement, since f_0 will be made to vary by the smallest mechanical vibrations.

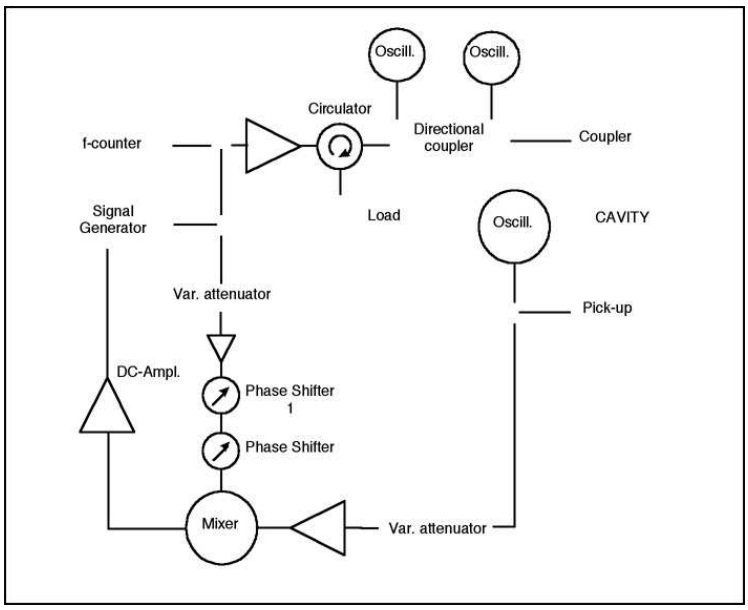

Fig. 5: Schematics of the phase-feedback control circuit for the Q_0 measurements of an SC cavity

A circuit similar to the one shown in Fig. 5 is used. A mixer compares the signal feeding the cavity (f_g) with that transmitted by the cavity. The two signals will have a phase difference θ bounded to the difference of frequency between the feeding signal and the actual resonant frequency (f_r) of the cavity:

$$tg\ \theta = \ Q(f_r/f_g)^2 \ (Q \text{ being the resonator quality factor}) \ .$$

If, at resonance, the phase difference between the two signals is set at $\pi/2$, small changes in the resonant frequency produce an output signal of the mixer which is proportional to the phase changes and, consequently, to the difference between the driving frequency and the resonant frequency. Such a signal, suitably amplified, can be used to modulate continuously the frequency output of the generator, keeping the $\omega = \omega_0$ condition locked.

5.4 Plotting quality factor versus accelerating field

As long as losses are ohmic at constant surface resistance, Q_0 is constant with increasing U (or E_{acc}), since $U/P_c = const.$

At high fields, however, losses tend to be non-ohmic. This is why it is necessary to measure Q_0 by the decay-time method at very low fields, i.e. to be sure to be in the region of purely ohmic losses.

Figure 6 shows a typical SC cavity performance curve, in which Q_0 is plotted versus the peak surface field. The significant Q_0 drop at high fields (accompanied by higher power dissipated by the cavity) is explained by field emission electron loading (see Section 6). Peak surface field (E_{pk}) and accelerating field (E_{acc}) are proportional to $\sqrt{U}$, through constants which are normally derived by appropriate simulation codes or bead pulling measurements. This defines the abscissa in the Q_0 vs. E_{acc} plot. Ordinate values (Q_0 at increasing fields) can be found by scaling the U/Pc ratio with the low-field Q_0 measured via stored-energy decay time.

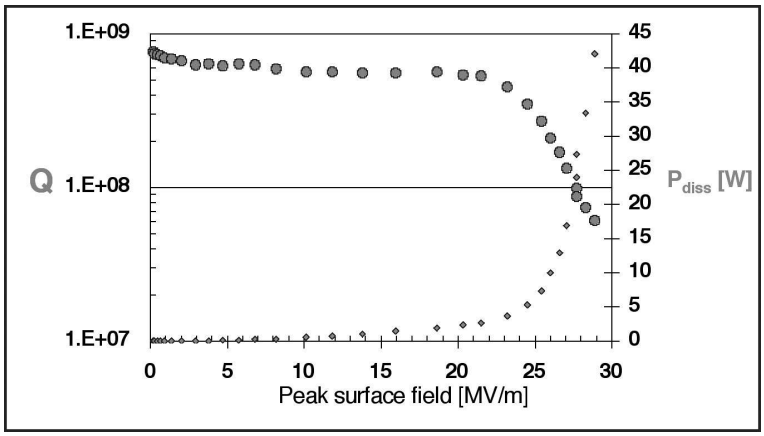

Fig. 6: Q_0 plotted against peak surface field: a typical example [19]

6 PRACTICAL LIMITATIONS TO ACHIEVABLE FIELDS

The theoretical maximum field limits, mainly correlated to the critical field of the superconductor, are not normally achievable in practical SC resonators. The various causes can be approximately grouped into (a) those which are correlated with the surface magnetic field (Section 6.1) and (b) those linked to the local electric field (Section 6.2).

Representatives of the first group are distributed anomalous losses connected to trapped magnetic flux or precipitated Nb hydrides, and local anomalous losses connected to the presence of defects on the cavity surface, driving to thermal breakdown.

Representatives of the second group are resonant field emission (also called 'multipacting') at relatively low EM fields, and non-resonant field emission at the highest fields.

6.1 Anomalous losses related to the surface magnetic field

6.1.1 Distributed losses related to a DC magnetic field

Distributed losses related to a DC magnetic field (like the Earth's magnetic field) give rise to an overall contribution to the surface resistance, which can be expressed by

$$R_{mag} = \frac{H_{ext}}{2H_{C2}} R_n \ , \tag{11}$$

R_n being the normal state resistance and H_{ext} the external magnetic field [20].

External magnetic field is expelled from the superconductor, except from the contribution given by distributed lattice defects or surface irregularities, which can act as distributed trapping sites.

If one takes the typical values for RRR = 300 Nb (H_{C2} = 2400 Oe and R_n = 1.5 mΩ at 1 GHz) the result is

$$R_{mag} = 0.3(\mathrm{n\Omega}) H_{ext}(\mathrm{mOe}) \sqrt{f(\mathrm{GHz})} \ .$$

These residual losses can be practically eliminated by providing proper shielding around the cavity and are not a fundamental problem.

6.1.2 Q-disease

Hydrogen is usually dissolved in the bulk of the newly bought material in negligible concentrations ($<$ 1 ppm wt). However, its concentration may be increased if, for example, the temperature rise during chemical etching is not kept below 20°C: in this case some ppm of H (by weight) can be present in the bulk.

Whereas at room temperature three orders of magnitude higher concentrations are necessary to form hydrides, a concentration of H of 2 ppm wt becomes critical below 150 K. Moreover, between 150 and 60 K the mobility of H is still quite significant, allowing the formation of sites of high hydrogen concentration. The part of the Nb hydride which forms on the surface exposed to RF fields can cause significant depression of the resonator Q even at quite low fields (Q-disease).

Two methods are known to prevent or avoid the problem. The first involves carefully heating the cavity up to 700–900°C to facilitate hydrogen outgassing as much as possible. The second requires cooling down the cavity more rapidly than the time necessary for H precipitation in the range 150 K to 60 K (1–2 hours are usually sufficient). Below 60 K the mobility of H becomes negligible and the new formation of hydride is no longer a concern.

6.1.3 Local defects

Local thermal breakdown starts at micrometric sites on the SC surface where the RF losses are much higher than those due to the surface resistance of the SC material.

While DC currents flow around defects, the reactive part of the impedance causes AC currents to also flow through a defect. Joule heating can locally increase the temperature. When the temperature at the defect border is higher than the critical field of the superconductor, the NC region grows in size, and for further increases of the applied EM fields a thermal instability may develop, eventually driving the whole resonator into the NC state (quench).

A quench is normally observed as a saw-tooth pattern in both the signal from the pick-up probe and the reflected signal during a Q-curve measurement carried out in critical coupling conditions. This shows that all the power is reflected once the thermal instability shows up, but goes back to its original value when the SC state is restored after some cooling of the resonator.

Typical local defects can originate from imperfections caused by EBW. Examples are microscopic holes on the welding path, and Nb material which evaporates from the weld and then condenses somewhere else on the cavity surface in the form of small spheres. Other causes are chemical residues, foreign-material inclusions (e.g. embedded abrasives, see Fig. 7) or simply micrometric particles which fall in a high-H field region during cleaning or assembling of the resonator (unless particular care is taken in these delicate phases, the number of these dust components increases).

The previously mentioned temperature-mapping technique can be applied to multicell cavities, or other cavities of simple geometry, to detect the position and the relevance of the effect of a particular defect. In fact this method is rarely adopted and the identification of the size and material of the defect can only be made by scanning-electron-microscope investigation of the suspected zone. This requires that the cavity be cut at the equator: another practice which one also tends to avoid on a production scale!

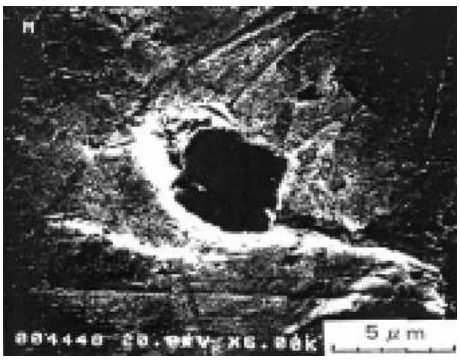

Fig. 7: Scanning-electron-microscope image of an embedded abrasive in a Nb surface [21]

6.1.4 Increasing the cavity RRR

A method often applied to increase H_{max} in the presence of small defects is to raise the thermal conductivity of Nb. As long as heat is transferred away from the location of the defect with more efficiency, it will be at higher local H-field (and corresponding E_{acc} field), such that the neighbouring SC material will exceed T_C.

The higher the RRR of the material, the higher its thermal conductivity κ. The formula

$$\kappa = \frac{RRR}{4}\left(\frac{W}{\mathrm{mK}}\right) \text{ [22]}$$

holds approximately; as a matter of fact, the correlation between electrical and thermal conductivity, which is well known for metals at room temperature, still holds true down to about 4 K, as long as electrons are still the dominant heat carriers. Below that temperature, at around 2 K, the density of phonons has a peak and lattice vibrations become the dominating phenomenon (at even lower temperatures the density of phonons also drops).

The RRR of Nb can be increased in several ways.

- Heating in very good vacuum up to $\sim 2000^\circ$C for some hours can outgas even O from the film and RRR = 1200 can be reached; however, the loss of mechanical properties and the risk to deform the resonator often make this a not very recommendable practice.
- Solid-state gettering is now widely applied: It consists in coating the exterior of a cavity with either yttrium or titanium, materials with a higher affinity to O than Nb, while warming up the resonator to 1200–1400°C to increase the mobility of O itself. Then the getter is removed by external chemical etching. RRR higher than 1000 can be obtained in this way.

With increasing RRR a linear increase was observed, over the last two decades, in the reachable accelerating gradient of SC structures, making it possible, nowadays, to exceed $E_{acc} = 30$ MV/m with $RRR \sim 300$. The main drawbacks of the RRR increase after cavity fabrication are an increase in the BCS surface resistance, due to increased electron mean free path (low-field Q-values by about a factor of two smaller should be expected), and a drop in the yield strength of the material following any of the heat treatments needed for this purpose.

6.1.5 Global heating

SC cavities based on films of either Pb or Nb deposited onto Cu substrates do not generally show any thermal breakdown limitations, due to the excellent thermal properties of the substrate.

Whether a resonator is made of an SC layer coated onto Cu or it is defect free, the ultimate observable behaviour is a global heating, supposedly driven by a large number of extremely small defects in high magnetic field regions. This can be distinguished from a local effect either via thermometry methods or via the observation of a Q-decrease with temperature increase (before any local quenches) and without photoemission (no FE).

6.2 Anomalous losses related to the surface electric field

The electric component of applied EM fields can also extract a large number of electrons from an SC surface, and they may absorb a large part of the power driven to the resonator.

Electron field emission can be either a resonant or a non-resonant phenomenon, the former being usually relevant for rather low EM fields, the latter being the practical cause of performance limitation for the largest number of SC resonators.

6.2.1 Resonant field emission (multipacting)

The resonant field emission (RFE) is a dissipative process preventing the resonator from increasing its energy in spite of the increase of the feeding power.

The phenomenon is triggered by a low-energy electron (few eV) which is released from the SC surface for some reason, such as photoemission, cosmic rays or electrons from non-resonant FE. The electron gets accelerated by the local electric field and can be bent back to the surface by the local magnetic field. On impact with the surface, this may cause the emission of other electrons, whose number depends basically on surface features, such as the emitting geometry and its coefficient of secondary-electron emission, and on the impact energy. As long as the coefficient is larger than one and the electrons hit the surface at the same EM field phase, with the same energy and approximately in the same region, the process leads to resonant multiplication of the number of electrons involved. An avalanche develops, which absorbs all the power additionally fed into the cavity, preventing the resonator stored energy from increasing and hence freezing the EM fields at the values that determine the resonant process (see Fig. 8).

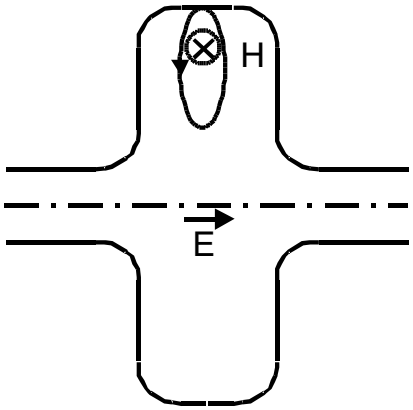

Fig. 8: Schematic of a first-order multipacting orbit. In one RF cycle the electron is bent back by the local electromagnetic fields onto the same emitting point, where it can extract secondary electrons and initiate an avalanche process.

Assuming that the electrons follow simple cyclotron orbits, the fundamental orbit frequency is $\omega_c \propto He/m$, H being the local magnetic field, e and m the electron charge and mass. To allow the resonant condition, H has to be such that emitted electrons are always in phase with the extracting EM field. The resonant condition can be satisfied clearly also for higher resonance orders: $\omega_g = n\omega_c$ (RFE of nth order).

These considerations explain why a number of RFE levels have usually to be overcome in a resonator. Of course the geometry of a cavity crucially affects the number of levels, their position versus input power and the ease with which they can be conditioned.

The coefficient of secondary-electron emission is peaked around 300–800 eV for most materials, while beyond 2000 eV it is lower than 1 for the large majority of them. That is the reason why RFE is a relatively low surface electric field phenomenon.

Ideal sites for RFE development are those regions in which the magnetic field does not vary significantly along the surface. Rounding off the equatorial region of multicell cavities to spherical (or elliptical) shape resulted in the complete elimination of multipacting, since the avalanche phenomenon is forced towards the equator line. This is where the magnetic field would allow RFE to develop, but the extracting electric field tends to zero, thus suppressing secondary electron multiplication.

Cleaning, baking, and applying gas discharges are known methods to reduce the secondary-electron coefficient. Furthermore, an RFE barrier is quite often overcome just by staying at an RFE level in high vacuum for minutes or hours (without any special discharge gas inlet).

RFE levels are easily recognisable in both steady-state and pulsed operation of the resonator, since one observes that the pickup signal on the oscilloscope remains locked at a certain level, while more power is driven from the input coupling line. One observes that the signal suddenly jumps to a higher value when the level is overcome (in some cases directly to the next level!). It is good practice to decrease the field to the same RFE level again and again until the level is actually cleaned. Computer-controlled procedures can replace the operator very efficiently and spare him this tedious work [23]. It is also advisable, whenever possible, to perform multipacting processing with the cavity in the NC state because of the larger resonator bandwidth and possible high power dissipation in the NC regime.

It should be finally mentioned that two-point multipacting has been observed when the resonance develops between two different points on the SC surfaces, e.g. mirror points around the equator in multicell cavities.

At present multipacting is not generally linked to the actual performance limitation of the cavity. It can be eliminated in multicell resonators by applying dedicated codes to find particular cavity shapes for which the phenomenon does not appear at all. However, it can still be an issue for low-β resonators, which can be described only by 3-D codes. In such a case the coarse definition of the EM fields makes it more difficult to determine the electron trajectories with sufficient accuracy. Hence there is no elegant means of trying to deal with RFE, other than to go through experimental tests. However, in most cases, RFE presents soft resonant levels, which can be overcome with properly devoted conditioning (taking maybe hours or days).

Nowadays RFE seems to play a more fundamental role in couplers, waveguide windows and coaxial lines (determining a maximum travelling-power limit) than in cavities themselves.

6.2.2 Non-resonant field emission: the phenomenon

The limit imposed by the Nb superheating field on the maximum achievable peak surface fields in β = 1 resonators is about 100 MV/m, which is still somewhat larger than the best updated performances ($\sim$ 80 MV/m). By far the most typical limiting mechanism to high fields in SC cavities is electron field emission (FE). In high electric field regions, electrons are emitted via quantum-mechanical tunnelling, which can dissipate a large part of the energy driven to the cavity. In some cases the limitation cannot be overcome, i.e. when the power absorbed by field-emitted electrons induces a quench.

The mechanism is usually explained by the modified Fowler–Nordheim (FN) equation, in which the emitted current density is given, in the RF regime, by [24]

$$J_{FN} = \frac{C}{\phi} S_{RF} (\beta_{RF} E_{RF})^{2.5} \exp\left(-\frac{B\phi^{3/2}}{\beta_{RF} E_{RF}}\right):$$

E_{RF} is the macroscopic electric field in V/m (i.e. assuming a smooth surface); ϕ is the material work function in eV; β_{RF} is the local field enhancement factor, which might be bound to the pin-like geometry of the emitting site (enhanced field emission – EFE); C is a constant which depends both on ϕ and β_{RF}; S_{RF} is the emitting area in m^2; and B is a numerical constant.

Some results show that at least half of FE sites can be well fitted with the modified FN law, whereas micron-sized particles are generally accepted to be the other most widely diffused cause of FE.

Field emitters vary substantially both in morphology and behaviour; hence, it is difficult to give a comprehensive description of the variety of experiments carried out so far on very different resonators. It is only possible to report here what are nowadays believed to be the most convincing explanations of the phenomenon.

First of all, the RF FE process has now largely been demonstrated to be similar to DC FE, except that the latter has an E^2 and not an $E^{2.5}$ dependence [25]: this resemblance induced many researchers to conduct experiments on the fundamental phenomena underlying FE in a DC regime. The onset time of

many discharges investigated in the DC regime was of the order of nanoseconds or less, with the initiation time decreasing with increasing field. These results are compatible with what would be allowed in the case of a typical SC RF cavity.

It was shown [26] that emission is certainly pushed to higher fields in a properly chemically etched surface, and that a high-RRR material and long (more than 3 h) heating at 1400°C can strongly reduce FE.

In some cases, the computed enhancement factors from FE current turned out to be much larger that the measured geometric irregularities of the surface in these regions. A micron-sized dust particle sitting on a geometric asperity was in similar cases proposed as an explanation (a multiplication of two enhancement factors $\beta_1\beta_2$ would be present). Where pure geometrical explanations fail, locally reduced work function (e.g. by contaminants) and the influence of the particle-substrate interface are proposed as a more complex explanation [26].

When the cause for FE appears clearly to be a foreign particle with poor thermal contact to the surface, thermionic emission (TE) is proposed as the explaining phenomenon [27], where the thermionic current density can be written as

$$J_{TE} = aE^2 \exp\left(-\frac{b}{E^2}\right).$$

Very revealing microscopic investigations of field emitters located by thermometry in 1.5 GHz cavities were done at Cornell [28], [29]. Emitters could be examined, at various processing stages, on the whole cavity surface (see also Fig. 9). It is deduced that the evolution of FE, increasing the applied field, consists of three phases:

- a pre-melting phase, in which FE is active, capable of degrading the Q, but where the current is still insufficient to melt the emitter;
- a melting phase, where the local E field is high enough that the current density exceeds about 10^{11} A/m^2 and the emission tip begins to melt;
- a third phase, in which the Joule losses of the emission current become so high that the emitter explodes and extinguishes.

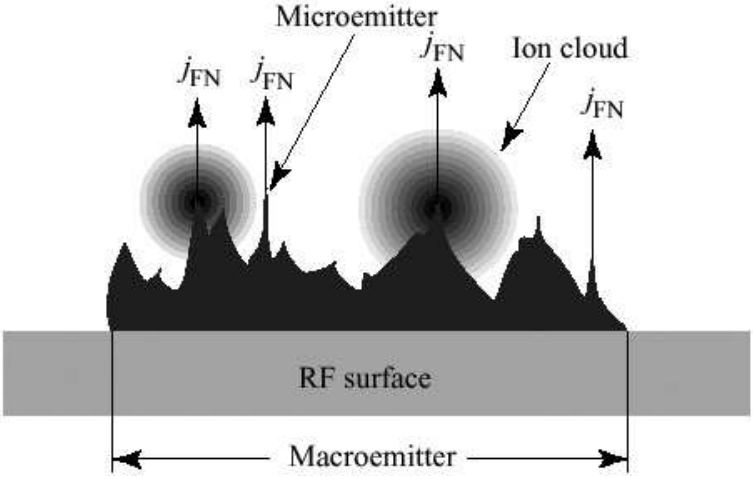

Fig. 9: Pictorial view of the macroemitter field-emission conditioning process, as proposed by J. Knobloch & H. Padamsee [29]

It is believed that initial electron emission causes, locally, sufficient heat to desorb gas, which is then ionized by the emission current. The ions are then accelerated towards the RF surface, thus reinforcing the process. The development of this large plasma would explain why melting phenomena are so much larger, in size, than the obviously small initial emitters.

6.2.3 Non-resonant field emission: the cures

Prevention is clearly the best cure for FE. This implies avoiding scratches or reducing their effect by means of a proper chemical treatment of the surface; on the other hand much effort is put into cleaning SC cavities prior to their installation, to minimize the number of particulate contaminants. The last step in cavity manipulation is an ultra-pure high-pressure rinsing with demineralized water (HPWR): this proved to be very effective in pushing the process to higher surface fields.

Before operating the cavity, RF processing can also be applied, with, for example, 60 kW/ 120 μs long pulses, allowing the necessary local current density for processing field emitters effectively to be provided. Gaseous He at a pressure around 5×10^{-5} Torr is often added to the FE conditioning recipe (He-conditioning). These processes lead to the destruction of FE sites and push the accelerating field further.

Perhaps the latest and most remarkable achievement, as far as overcoming FE is concerned, is the demonstration that 'nowadays' careful electropolishing (EP) allows the highest accelerating gradients by far to be reached and that it is superior to chemical polishing in the last treatment step. The formula for success, originally applied at KEK [15] and then adopted by other laboratories, is approximately the following: half-cell annealing (at 1440°C with Ti cage), followed by BCP and 100 μm EP. Annealing at 750°C and high-pressure rinsing complete the treatment. Acceptable drawbacks are that EP is somewhat slower than BCP (0.4 versus 1–2 μm/min) and that subsequent annealing is needed to outgas hydrogen, which is otherwise trapped in the bulk material during EP and can give rise to Q-disease.

7 STATE OF THE ART

Superconducting resonators have now been extensively adopted for the most various applications, from low-β heavy-ion linacs, to high-energy and high-current storage rings, recirculating linacs and free-electron lasers. The resonator developments are still very pronounced and this is the major reason why new projects have been funded or are proposed for funding.

I would like to recall here only those work-in-progress issues which look most striking to me.

7.1 Highest achievable gradients

The steady increase in the accelerating field has been impressive. Ten years ago $E_{acc} \sim 7$ MV/m was the limit. But then 10 MV/m was reached at TJNAF in Virginia, USA in 1992, 16.7 MV/m in 1996 and 23.9 MV/m in 1997 at DESY, Germany. While the present performances of multicell cavities seem to have settled around 25 to 30 MV/m worldwide, a recent jump in single-cell cavity field beyond 40 MV/m was obtained by means of electropolishing (pioneered at KEK, Japan and soon followed by many others). It remains to be seen whether (or when) this technology will also prompt a jump in the performance of multicell cavities.

For a very long time, the community of SC heavy-ion resonators has demonstrated its ability to reach, in a reproducible way, peak surface fields in excess of 50 MV/m (corresponding to $E_a \sim 25$ MV/m for $\beta = 1$ cavities). It should be emphasised that extreme performances have never been its main goal.

7.2 Reproducibility of excellent results

Beyond world records, it is crucial to demonstrate that the best results can be obtained with a large number of resonators, meaning that the various technological steps are under firm control.

This was demonstrated for example at TJNAF: The machine was designed for average accelerating fields of about 7 MV/m, but it has now been demonstrated that all their numerous cavities can reach fields between 25 and 30 MV/m very reliably. The same can be said with the experience gained by the TESLA test facility developments, with the additional merit that the goal of average fields between 20

and 30 MV/m has been reached through the technological transfer of the resonator production to several industries in different European countries.

7.3 New applications and new resonator shapes

The interest in intense proton accelerators for the treatment of nuclear waste, materials research and energy production has triggered the development of multicell resonators. These include modified shapes (matched for β-values from 0.5 to 0.8) [30–32] or rather old cavity shapes whose development had been left in an initial phase (spoke resonators [33] or re-entrant cavities [34], [35]). These resonators are susceptible to appreciable gradient increase in the next few years.

In the low-β cavity community, the development, construction and tests of SC RF Quadrupoles (RFQs) represent an extreme of complexity in the successful development of the technology of full Nb [19]. They feature a very large number of EBW joints and extremely high accuracy is required in the positioning of the RFQ electrodes (see Fig. 10).

7.4 Cost-reducing technologies

Last but not least, one should mention those technologies, the development of which would imply a significant cost reduction in the production of a large number of cavities. The proposed SC linear collider TESLA aims at producing 20 000 nine-cell resonators (obviously on an industrial scale): all R&D steps in the cost-cutting direction increase the probability of approval of that project. The technology of Nb sputtered onto Cu resonators is extremely interesting in order to minimize the amount of Nb used. The problems of the rather steep Q_0 drop at high fields must be solved. The development of hydroformed or spun resonators would be extremely valuable to eliminate the expensive EBW of multicell-cavity parts, once high E_{acc} values have been reliably reached. It should be emphasized that some multicell-spun resonators already exceed 30 MV/m, after significant chemical polishing (see Fig. 11). EP might also prove to be beneficial in this case.

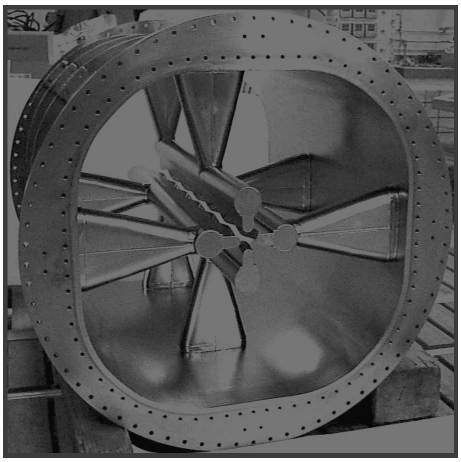

Fig. 10: The recently built and tested SC RF Quadrupole, part of the SC heavy-ion injector at INFN-LNL, exceeded a peak surface field of 28 MV/m CW and showed excellent alignment of the electrodes [19]

Hydroformed single-cell resonators very recently exceeded $E_{acc} \sim 40$ MV/m (once EP had been done at the end of the cavity treatment) [37]. Successful hydroforming of multicell cavities might follow quite soon.

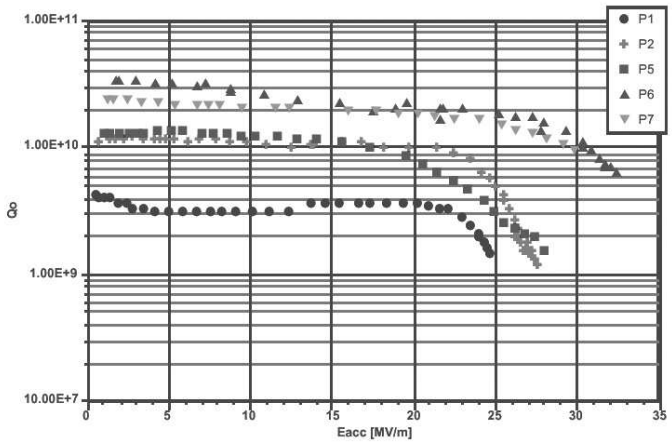

Fig. 11: Summary of the best performances achieved with five seamless monocell cavities made from high-purity niobium of $RRR \geq 250$. All Q_0 vs. E_{acc} dependencies are taken at a temperature of 2 K [36].

Acknowledgement

I wish to thank Anna Maria Porcellato for her critical revision of this manuscript.

REFERENCES

[1] H. Lengeler, CERN Accelerator School, Superconductivity in Particle Accelerators, CERN 89–04, pp. 197–229.

[2] V. Palmieri, Superconductivity, these proceedings.

[3] H. Padamsee, J. Knobloch and T. Hays, *RF Superconductivity for Accelerators* (John Wiley and Sons, New York, 1998).

[4] H. Lengeler *et al., IEEE Trans. Magn.* **MAG-21** (1985) 1014.

[5] M. Tigner and H. Padamsee, Cornell CNLS 82/553.

[6] P. Kneisel, Ti-gettering.

[7] K.W. Shepard, *Nucl. Instrum. Methods* **A382** (1996) 125.

[8] C. Benvenuti *et al.*, Proc. 8th Workshop on RF Superconductivity, Abano Terme (Padova, Italy), 6–10 October 1997, p. 1038.

[9] C. Benvenuti, N. Circelli, M. Hauer, *Appl. Phys. Lett.* **45** (1984) 583.

[10] S. Stark *et al.*, Proc. 8th Workshop on RF Superconductivity, Abano Terme (Padova, Italy), 6–10 October 1997, p. 1156.

[11] B. Bonin, CERN Accelerator School, Superconductivity in Particle Accelerators, CERN 96–03, p. 191.

[12] C.Z. Antoine *et al.*, Proc. 8th Workshop on RF Superconductivity, Abano Terme (Padova, Italy), 6–10 October 1997, p. 598.

[13] V. Palmieri, Proc. 8th Workshop on RF Superconductivity, Abano Terme (Padova, Italy), 6–10 October 1997, p. 553.

[14] P. Kneisel and B. Lewis, Proc. 7th Workshop on RF Superconductivity, Gif-sur-Yvette (France), October 1995, p. 311.

[15] K. Saito *et al.*, Proc. 8th Workshop on RF Superconductivity, Abano Terme (Padova, Italy), 6–10 October 1997, p. 553.

[16] C. Lyneis *et al.*, Proc. 1972 Proton Linear Accelerator Conference, LANL, Los Alamos (1972), 98.

[17] J. Knobloch *et al., Rev. Sci. Instrum.* **65** (1995) 3251.

[18] H. Padamsee, J. Knobloch and T. Hays, *RF Superconductivity for Accelerators* (John Wiley and Sons, New York, 1998), p. 145.

[19] G. Bisoffi *et al.*, Proc. 7th European Particle Accelerator Conference, in press.

[20] H. Padamsee, J. Knobloch and T. Hays, *RF Superconductivity for Accelerators* (John Wiley and Sons, New York, 1998), p. 174.

[21] H. Kitamura *et al.*, Proc. 8th Workshop on RF Superconductivity, Abano Terme (Padova, Italy), 6–10 October 1997, p. 667.

[22] H. Padamsee *et al.*, Proc. '1991 Electron Beam Melting and Refining Conference', November 1991.

[23] S. Canella *et al.*, Proc. 5th European Particle Accelerator Conference, Barcelona (Spain), 10–14 June 1996, p. 2109.

[24] J. Tan *et al., J. Phys. D: Appl. Phys.* **27** (1994) 2644.

[25] J. Tan, Proc. 7th Workshop on RF Superconductivity, Gif-sur-Yvette (France), 17–20 October 1995, p. 105.

[26] N. Pupeter *et al.*, Proc. 7th Workshop on RF Superconductivity, Gif-sur-Yvette (France), 17–20 October 1995, p. 67.

[27] M. Pekeler *et al.*, Proc. of the 7th Workshop on RF Superconductivity, Gif-sur-Yvette (France), 17–20 October 1995, p. 79.

[28] J. Knobloch, Proc. 7th Workshop on RF Superconductivity, Gif-sur-Yvette (France), 17–20 October 1995, p. 95.

[29] J. Knobloch and H. Padamsee, Proc. 8th Workshop on RF Superconductivity, Abano Terme (Padova, Italy), 6–10 October 1997, p. 994.

[30] C. Benvenuti *et al.*, Proc. 8th Workshop on RF Superconductivity, Abano Terme (Padova, Italy), 6–10 October 1997, p. 1038.

[31] H. Safa, Proc. 9th Workshop on RF Superconductivity, Santa Fe, NM (USA), 1–5 November 1999, in press.

[32] C. Pagani, Proc. 9th Workshop on RF Superconductivity, Santa Fe, NM (USA), 1–5 November 1999, in press.

[33] J.R. Delayen *et al.*, Proc. 1992 Linear Accelerator Conference, 24–28 August 1992, Ottawa (Canada), p. 695.

[34] P.H. Ceperly *et al., Nucl. Instrum. Methods* **136** (1976) 421.

[35] A. Pisent *et al.*, Proc. 7th European Particle Accelerator Conference, in press.

[36] P. Kneisel, V. Palmieri and K. Saito, Proc. 9th Workshop on RF Superconductivity, Santa Fe, NM (USA), 1–5 November 1999, in press.

[37] W. Singer *et al.*, Proc. 7th European Particle Accelerator Conference, in press.